

Observation of the $^1S_0 \rightarrow ^3P_0$ clock transition in $^{27}\text{Al}^+$

T. Rosenband,^{1,*} P. O. Schmidt,^{1,†} D. B. Hume,¹ W. M. Itano,¹ T. M. Fortier,² J. E. Stalnaker,¹ S. A. Diddams,¹ J. C. J. Koelemeij,^{1,‡} J. C. Bergquist,¹ and D. J. Wineland¹

¹*National Institute of Standards and Technology, 325 Broadway, Boulder, CO 80305*

²*Los Alamos National Laboratory, P-23 Physics Division, Los Alamos, NM 87545*

(Dated: February 9, 2014)

We report for the first time, laser spectroscopy of the $^1S_0 \rightarrow ^3P_0$ clock transition in $^{27}\text{Al}^+$. A single aluminum ion and a single beryllium ion are simultaneously confined in a linear Paul trap, coupled by their mutual Coulomb repulsion. This coupling allows the beryllium ion to sympathetically cool the aluminum ion, and also enables transfer of the aluminum's electronic state to the beryllium's hyperfine state, which can be measured with high fidelity. These techniques are applied to a measurement of the clock transition frequency, $\nu = 1\,121\,015\,393\,207\,851(8)$ Hz. They are also used to measure the lifetime of the metastable clock state, $\tau = 20.6 \pm 1.4$ s, the ground state 1S_0 g-factor, $g_S = -0.00079248(14)$, and the excited state 3P_0 g-factor, $g_P = -0.00197686(21)$, in units of the Bohr magneton.

PACS numbers:

The $^1S_0 \rightarrow ^3P_0$ transition in Al^+ has long been recognized as a good clock transition [1, 2], due to its narrow natural linewidth (8 mHz), and its insensitivity to magnetic fields and electric field gradients ($J = 0$), which are common in ion traps. More recently, this transition was also found to have a small room-temperature blackbody radiation shift [3]. However, difficulties with direct laser cooling and state detection have so far prevented its use.

Some of the basic ingredients for ion-trap based quantum computing [4] can be used to overcome these difficulties with the method of quantum logic spectroscopy [5], where an auxiliary ion takes over the requirements of laser cooling and state detection. Quantum logic spectroscopy was first demonstrated experimentally on the $^1S_0 \rightarrow ^3P_1$ transition in $^{27}\text{Al}^+$ [6]. Here we use this technique for spectroscopy of the narrow $^1S_0 \rightarrow ^3P_0$ clock transition, allowing, for the first time, high precision optical spectroscopy of an atomic species that can not be directly laser cooled.

With the advent of octave-spanning Titanium:Sapphire femtosecond laser frequency combs [7, 8], optical atomic frequency standards can be compared with an uncertainty limited only by quantum projection noise [9] and the systematic errors of the atomic standards. This stability and accuracy can be transferred to any part of the optical spectrum, as well as the RF domain. The $^1S_0 \rightarrow ^3P_0$ clock transition in $^{27}\text{Al}^+$, due to its insensitivity to external fields, is a viable candidate to reach 10^{-18} inaccuracy. Here we demonstrate high precision spectroscopy of the clock transition in a single $^{27}\text{Al}^+$ ion, which is the fundamental step necessary to realize such a frequency standard.

We use $^{27}\text{Al}^+$, because this is the only naturally occurring isotope of aluminum. With nuclear spin $I = \frac{5}{2}$, $^{27}\text{Al}^+$ has no first-order magnetic-field-independent transition, but this is not a significant drawback. Instead, we create a “virtual” ($^1S_0, m_F = 0$) \rightarrow ($^3P_0, m_{F'} = 0$) field-

independent transition, by regularly alternating between ($m_F = -\frac{5}{2}$) \rightarrow ($m_{F'} = -\frac{5}{2}$) and ($m_F = \frac{5}{2}$) \rightarrow ($m_{F'} = \frac{5}{2}$) transitions [10]. This way, the average Zeeman state of both the ground and excited clock state is strictly zero. A benefit of this approach is that the outer $m_F = \pm\frac{5}{2}$ states can be prepared more easily than the inner m_F states, by optical pumping through the ($^3P_1, F = \frac{7}{2}$) state (300 μs lifetime). In addition, the ion's Zeeman splitting serves as a real-time magnetometer to determine the quadratic Zeeman shift of the clock transition.

In the experiment, single $^9\text{Be}^+$, and $^{27}\text{Al}^+$ ions are loaded into a linear Paul trap [11], by electron impact ionization. Under ultra-high vacuum conditions, one ion pair usually lasts for several hours, before an adverse chemical reaction with background gas removes one of the ions from the trap. The pair forms a two-ion “crystal” along the trap axis, whose in-phase-motion axial normal mode frequency is 2.62 MHz. The radial modes (perpendicular to the trap axis), where the $^{27}\text{Al}^+$ ion's amplitude is largest, have frequencies of 3.8 MHz and 4.9 MHz. Laser beams of 313 nm wavelength drive Doppler cooling, stimulated Raman, and repumping transitions on $^9\text{Be}^+$ [12]. Another laser produces 266.9 nm radiation to drive the ($^1S_0, F = \frac{5}{2}$) \rightarrow ($^3P_1, F = \frac{7}{2}$) transition in $^{27}\text{Al}^+$, and a frequency-quadrupled fiber laser at 267.4 nm (the clock laser), with approximately 3 Hz linewidth, excites the $^1S_0 \rightarrow ^3P_0$ transition.

The $^1S_0 \rightarrow ^3P_0$ transition is probed with single interrogation pulses from the clock laser. Since the upper state is metastable, the method of electron-shelving detection [1] is applied. This way the $^1S_0 \rightarrow ^3P_1$ transition is modulated by the clock states, and the modulation condition (allowed or forbidden) is detected with quantum logic.

Quantum logic spectroscopy of the $^1S_0 \rightarrow ^3P_1$ transition has been described previously [6], and is used similarly here. A quantum logic pulse sequence (described below) maps the $^{27}\text{Al}^+ ^1S_0$ state to the dark $^9\text{Be}^+ F$

= 1 hyperfine ground state via a $^1S_0 \rightarrow ^3P_1$ motional-sideband excitation. This sequence is blocked when the $^{27}\text{Al}^+$ ion is in the 3P_0 state, leaving $^9\text{Be}^+$ in the bright $F = 2$ hyperfine ground state, into which it had previously been optically pumped. An average of seven $^9\text{Be}^+$ 313 nm fluorescence photons are counted if the $^{27}\text{Al}^+$ ion is in the 3P_0 state (Figure 1b), and only one photon is counted if the $^{27}\text{Al}^+$ ion is in the 1S_0 state (Figure 1a). This provides for clock-state discrimination with 80 % fidelity in a single detection experiment, limited by inaccuracies in the various π -pulses, and imperfect ground-state cooling. However, the single-experiment detection fidelity does not significantly affect the final detection fidelity for the clock state. We simply repeat the readout sequence several times, and the combined information allows nearly unit detection fidelity [13].

A typical ($^1S_0, m_F = \frac{5}{2}$) \rightarrow ($^3P_0, m_{F'} = \frac{5}{2}$) interrogation consists of the following steps, with specified durations. For $m_F = m_{F'} = -\frac{5}{2}$, the polarizations and angular momentum states of Al^+ are reversed.

1. Sympathetic Doppler cooling via $^9\text{Be}^+$ (600 μs) cools all six normal modes of the two-ion crystal to the Doppler limit (mean motional quantum number $\bar{n} \approx 3$).
2. Clock interrogation (1 to 100 ms pulse duration, adjusted for desired resolution) drives the $^1S_0 \rightarrow ^3P_0$ transition. Beryllium Doppler cooling light is applied simultaneously to counteract anomalous heating of the ions [14, 15].

Subsequently, state detection (1S_0 or 3P_0) is performed by repeating the following sequence about 10 times.

1. Optical pumping π -pulse $^{27}\text{Al}^+$ ($^1S_0, F = \frac{5}{2}, m_F = \frac{3}{2}$) \rightarrow ($^3P_1, F = \frac{7}{2}, m_{F'} = \frac{5}{2}$) (4 μs) transfers residual inner Zeeman state population to the outer $m_F = \frac{5}{2}$ state. The inner states may be populated due to spontaneous decay from the 3P_0 state, or due to imperfect polarization and off-resonant transitions during other $^1S_0 \rightarrow ^3P_1$ pulses. Most of the time this pulse has no effect, because $^{27}\text{Al}^+$ is already in the ($^1S_0, m_F = \frac{5}{2}$) state.
2. Sympathetic Doppler cooling (600 μs).
3. Ground-state cooling of the axial modes of the two-ion crystal (1 ms), $\bar{n} < 0.05$ [16].
4. BSB π -pulse $^{27}\text{Al}^+$ ($^1S_0, F = \frac{5}{2}, m_F = \frac{5}{2}$) \rightarrow ($^3P_1, F = \frac{7}{2}, m_{F'} = \frac{7}{2}$) (30 μs).
5. RSB π -pulse $^9\text{Be}^+$ ($^2S_{1/2}, F = 2, m_F = -2$) \rightarrow ($^2S_{1/2}, F = 1, m_F = -1$) (7 μs).
6. Detection on the Be^+ cycling transition (200 μs) ($^2S_{1/2}, F = 2, m_F = -2$) \rightarrow ($^2P_{3/2}, F = 3, m_F = -3$). In the $F = 2$ state, Be^+ fluoresces strongly,

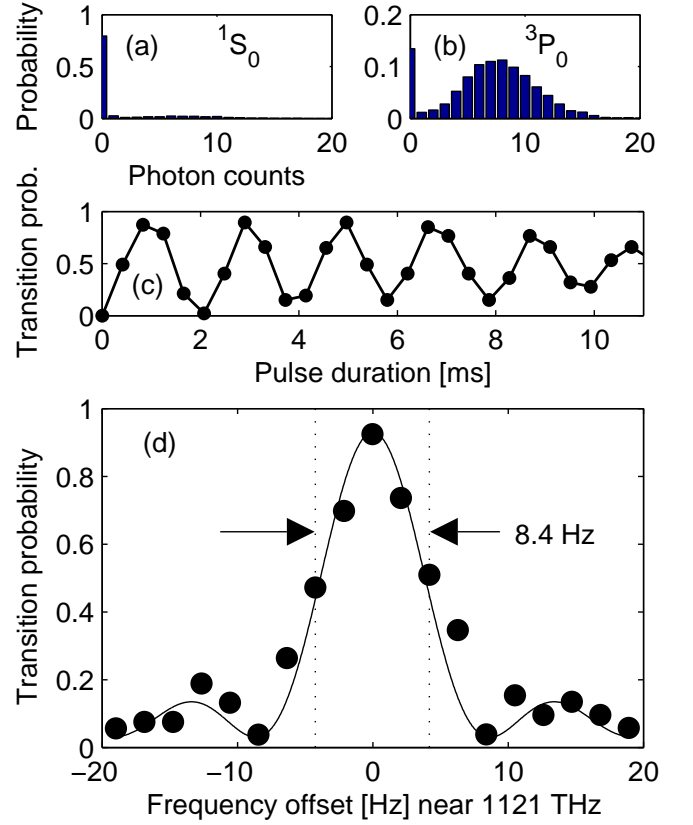


FIG. 1: Histograms of photon counts used for discrimination of 1S_0 (a) and 3P_0 (b) states in Al^+ via Be^+ fluorescence (see text). (c) Rabi flopping averaged over forty scans of the $^1S_0 \rightarrow ^3P_0$ probe time (0-11 ms). Lines are drawn to guide the eye. (d) Average transition probability of fifty frequency scans across the ($^1S_0, m_F = \frac{5}{2}$) \rightarrow ($^3P_0, m_{F'} = \frac{5}{2}$) resonance in Al^+ . Each measurement consists of one 3P_0 interrogation (100 ms probe time), followed by 5 to 10 state-detection repetitions (10 to 20 ms total). The fitted curve is a Fourier-limited Rabi lineshape, scaled to the observed 90 % contrast.

and it is dark in the $F = 1$ state (see Fig. 1a and 1b).

Because the duration of each state detection repetition is about 2 ms, excitations into the 3P_1 state (300 μs lifetime) usually decay back to the 1S_0 state, allowing re-excitation, while 3P_0 excitations (20.6 s lifetime) are unlikely to change during the detection sequence.

For every clock interrogation pulse, the sequence of photon counts in step 6 is recorded by a computer, which performs a maximum-likelihood analysis to determine whether the Al^+ ion was in the 1S_0 or 3P_0 state [13]. Transitions between the two states are detected, and multiple repetitions of the same experiment yield the transition probability. It should be noted that the ion may be in the 1S_0 or 3P_0 state at the beginning of each experiment, depending on the outcome of the previous experiment [17]. The final signal is the computer's deter-

mination of whether or not the ion has made a transition. Figures 1c and 1d show Rabi flopping, and a scan of the clock laser frequency across the $^1S_0 \rightarrow ^3P_0$ resonance, with this method.

When performing an absolute frequency measurement of the $^1S_0 \rightarrow ^3P_0$ transition, the linear Zeeman splitting of several 10^4 Hz/mT (see below) in both the ground and excited clock states must be accounted for. To achieve first-order field insensitivity, we create a virtual $m_F = 0$ transition by alternating between states of opposite angular momentum, and tracking separately the mean and difference frequencies of the two transitions [10]. The mean frequency has no linear dependence on the magnetic field, although a quadratic Zeeman shift of -70 Hz/mT² remains [18]. The difference frequency is directly proportional to the magnetic field, providing a real-time field measurement. In this way, the linear Zeeman effect does not shift the clock's center frequency, while the quadratic Zeeman shift can be determined from the linear splitting and accounted for with submillihertz inaccuracy.

To lock the laser frequency to the atomic reference, the laser's frequency offset from the atomic resonance is regularly measured and corrected. Frequency corrections are obtained by alternating between the left and right "half-power" points of the ion's resonance and applying frequency feedback to keep the transition probabilities equal. In order to switch between angular momentum states, a computer-controlled waveplate selects purely σ_+ or σ_- -polarized $^1S_0 \rightarrow ^3P_1$ light that optically pumps $^{27}\text{Al}^+$ to the $m_F = \pm \frac{5}{2}$ ground states. At the operating field of approximately 0.1 mT, and typical Fourier limited linewidths of 20 Hz or less, the linear Zeeman structure of both clock states is well resolved. A synthesizer driven acousto-optic frequency shifter changes the probe frequency by $\Delta f \approx -4$ kHz to drive the $(^1S_0, m_F = \frac{5}{2}) \rightarrow (^3P_0, m_{F'} = \frac{5}{2})$ transition, and by $-\Delta f$ to drive the opposite Zeeman states. When locking the clock laser to the atomic transition, the clock ground state is switched between the $m_F = \pm \frac{5}{2}$ states every three seconds. This way, magnetic field fluctuations (typically below 100 nT in several minutes) contribute only short-term instability in the clock frequency, rather than long-term inaccuracy.

We have locked the clock laser to the virtual $m_F=0$ clock transition as described above and used the fourth subharmonic at 1070 nm to reference one tooth of an octave-spanning Titanium:Sapphire femtosecond laser frequency comb (femtosecond-comb) [19]. The offset frequency of the femtosecond-comb is locked by use of an f-2f interferometer, and the repetition rate is measured by a hydrogen maser referenced to the NIST-F1 primary cesium standard [20]. A 2600 second long measurement of the $^{27}\text{Al}^+$ clock transition frequency yields $\nu = 1\,121\,015\,393\,207\,851(8)$ Hz, where the uncertainty is dominated by short-term frequency fluctuations in the hydrogen maser. Systematic uncertainties in Al^+ are not expected to be significant at this level, where the largest

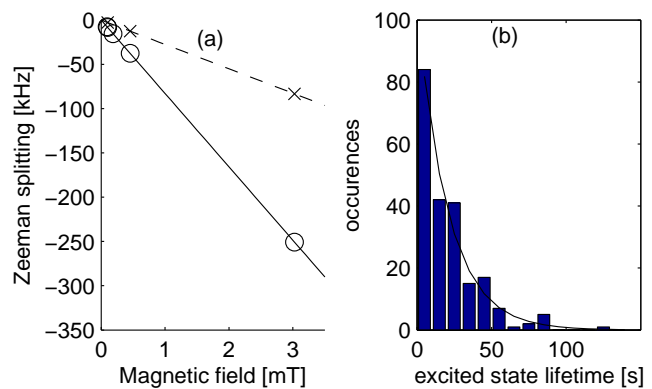


FIG. 2: Linear Zeeman splitting (a) of the $(m_F = \pm \frac{5}{2}) \rightarrow (m_{F'} = \pm \frac{5}{2})$ transition pair (o) and the $(m_F = \pm \frac{5}{2}) \rightarrow (m_{F'} = \pm \frac{3}{2})$ transition pair (x). Straight lines correspond to the reported g-factor differences. Histogram of lifetimes (b) of 215 decays from the 3P_0 state. The curve shows the expected number of decays for a lifetime $\tau = 20.6$ s.

terms are second-order Doppler shifts of approximately 0.03 Hz.

We have also measured the Landé g-factors of the 1S_0 and 3P_0 states. Interrogation pulses (π -polarized) yield the g-factor difference $g_P - g_S$ [21], where g_P and g_S are the g-factors of the 3P_0 and 1S_0 states, respectively. In addition we use $\sigma_{+/-}$ -polarized interrogation pulses to measure another, linearly independent combination of g_P and g_S , providing an accurate measurement of both g-factors, which is unaffected by the chemical shifts that currently limit the accuracy of nuclear magnetic resonance (NMR) based measurements of g_S [22]. An external magnetic field B splits the $m_F = \pm \frac{5}{2}$ transition frequencies by $\Delta\nu = 5B(g_P - g_S)\mu_B$, where μ_B is the Bohr magneton. The frequency splitting $\Delta\nu$ is tracked and recorded automatically in the clock laser lock described above. In order to measure the magnetic field, we use the simultaneously trapped Be^+ ion. Be^+ has well known ground-state Zeeman splitting [23], allowing for accurate calibration of the external magnetic field. In between aluminum clock interrogations, a 1.25 GHz magnetic field is applied to the beryllium ion with a loop antenna. Computer control software adjusts the radiation frequency to drive and track the magnetic-field-sensitive $(^2S_{1/2}, F = 2, m_F = -2) \rightarrow (^2S_{1/2}, F = 1, m_F = -1)$ transition, establishing a record of the magnetic field. We find the Zeeman splitting of $^{27}\text{Al}^+$ to be $\Delta\nu/B = -82884(5)$ Hz/mT, or $g_P - g_S = -0.00118437(8)$ (see Figure 2a). A recent multi-configuration Dirac-Hartree-Fock calculation [18] yields a similar theoretical value of $g_P - g_S = -0.00118(6)$.

In order to determine separate values g_P , and g_S , we repeated the above experiment with $\sigma_{+/-}$ -polarized clock radiation. This way, the $(^1S_0, m_F = -\frac{5}{2}) \rightarrow (^3P_0, m_{F'} = -\frac{3}{2})$, and $(^1S_0, m_F = \frac{5}{2}) \rightarrow (^3P_0, m_{F'} = \frac{3}{2})$ transitions are probed, and their magnetic-field-induced split-

ting $\Delta\nu'$ is measured. From $\Delta\nu'/B = (3g_P - 5g_S)\mu_B = -27547(5)$ Hz/mT we find $g_P = -0.00197686(21)$ and $g_S = -0.00079248(14)$. The uncertainties of these values are dominated by inaccuracies in the $^9\text{Be}^+$ -based magnetic field calibration. This was caused by a perturbation of the current supply for the DC magnetic field from the 1.25 GHz RF pulse itself. We estimate that this perturbation is 21 ± 200 nT in both the π and $\sigma_{+/-}$ measurements, and derive the stated uncertainties from the measurements at 3 mT, where the magnetic field uncertainty has the smallest effect on our results.

Since g_S depends solely on the ion's shielded nuclear magnetic moment, this measurement may be compared with the value recorded in nuclear data tables, which stems from NMR experiments. An estimated shielding factor of $\sigma = 7.87(39) \times 10^{-4}$ [18] for $^{27}\text{Al}^+$, leads to a bare moment of $\mu_N = 3.64067(28)$ nuclear magnetons. This differs from the published value of $\mu_N = 3.64150687(65)$ [24] by $0.00084(28)$. However, the liquid-state NMR result does not account for the chemical shift of the nuclear magnetic moment due to the aqueous solution, which generally has a magnitude of $10^{-4} - 10^{-3}$ nuclear magnetons [22].

Hyperfine-induced spontaneous decay rates of $^3\text{P}_0$ states for the Mg-isoelectronic sequence have been calculated [25]. More recently, the lifetime was calculated [18] as 22.7 ± 4 s. Here we measured the lifetime by repeatedly exciting the $^3\text{P}_0$ state and waiting for spontaneous decay into the ground state [26]. The aluminum internal state was monitored by continuously applying the previously described clock state readout sequence. Once decay has been detected, the ion is re-excited. A total of 215 spontaneous emission events were observed this way, with a mean lifetime $\tau = 20.6 \pm 1.4$ s. The reported uncertainty is statistical, and systematic biases are estimated to be less than 0.25 s. Figure 2(b) shows the distribution of decay times.

In conclusion, we have demonstrated high resolution spectroscopy of the $^1\text{S}_0 \rightarrow ^3\text{P}_0$ clock transition in $^{27}\text{Al}^+$ using quantum logic. This technique was used to measure the clock transition frequency with a fractional uncertainty of 7×10^{-15} . We have also calibrated the g-factors of the ground and excited states and measured the excited state lifetime. These are the basic steps necessary to implement an accurate frequency standard based on $^{27}\text{Al}^+$.

We acknowledge support from ONR and DTO. We thank V. Meyer for constructing the ion trap used for these experiments, and E. A. Donley, J. Ye, M. A. Lombardi, and D. R. Smith for their careful reading of this manuscript. The authors are grateful to T. Parker, S. Jefferts and T. Heavner for providing the absolute frequency calibration. This work is a contribution of NIST,

and is not subject to U.S. copyright.

* trosen@boulder.nist.gov

† Supported by the Alexander von Humboldt Foundation; Present address: Institut für Experimentalphysik, Universität Innsbruck, Austria

‡ Supported by the Netherlands Organisation for Scientific Research (NWO); Present address: Institut für Experimentalphysik, Heinrich-Heine-Universität Düsseldorf, Germany

- [1] H. G. Dehmelt, IEEE Trans. Inst. Meas. **31**, 83 (1982).
- [2] N. Yu, H. Dehmelt, and W. Nagourney, in *Proc. Nat. Acad. Sci* (1992), p. 7289.
- [3] T. Rosenband, et al., arXiv:physics/0611125 (v1 14 Nov 2006).
- [4] J. I. Cirac and P. Zoller, Phys. Rev. Lett. **74**, 4091 (1995).
- [5] D. J. Wineland, J. C. Bergquist, J. J. Bollinger, R. E. Drullinger, and W. M. Itano, in *Proceedings of the 6th Symposium on Frequency Standards and Metrology*, edited by P. Gill (World Scientific, 2002), pp. 361–368.
- [6] P. O. Schmidt, et al., Science **309**, 749 (2005).
- [7] S. A. Diddams, et al., Phys. Rev. Lett. **84**, 5102 (2000).
- [8] T. Udem, R. Holzwarth, and T. W. Hänsch, Nature **416**, 233 (2002).
- [9] W. M. Itano, et al., Phys. Rev. A **47**, 3554 (1993).
- [10] J. E. Bernard, L. Marmet, and A. A. Madej, Opt. Comm. **150**, 170 (1998).
- [11] M. A. Rowe, et al., Quant. Inform. Comp. **2**, 257 (2002).
- [12] C. Monroe, et al., Phys. Rev. Lett. **75**, 4011 (1995).
- [13] *To be published.*
- [14] Q. A. Turchette, et al., Phys. Rev. A **61**, 063418 (2000).
- [15] L. Deslauriers, et al., Phys. Rev. Lett. **97**, 103007 (2006).
- [16] M. D. Barrett, et al., Phys. Rev. A **68**, 042302 (2003).
- [17] W. Nagourney, N. Yu, and H. Dehmelt, Opt. Comm. **79**, 176 (1990).
- [18] W. M. Itano, *unpublished calculation* (2006).
- [19] T. M. Fortier, A. Bartels, and S. A. Diddams, Opt. Lett. **31**, 1011 (2006).
- [20] T. P. Heavner, S. R. Jefferts, E. A. Donley, J. H. Shirley, and T. E. Parker, IEEE Trans. Inst. Meas. **54**, 842 (2005).
- [21] M. M. Boyd, et al., Science **314**, 1430 (2006).
- [22] M. G. H. Gustavsson and A.-M. Mårtensson-Pendrill, Phys. Rev. A **58**, 3611 (1998).
- [23] D. J. Wineland, J. J. Bollinger, and W. M. Itano, Phys. Rev. Lett. **50**, 628 (1983).
- [24] P. Raghavan, At. Data Nucl. Data Tables **42**, 189 (1989).
- [25] T. Brage, P. G. Judge, A. Aboussaid, M. R. Godefroid, P. Jönsson, A. Ynnerman, C. F. Fischer, and D. S. Leckrone, Astrophys. J. **500**, 507 (1998). These results contain a typographical error. The $\text{Al}^+ \ ^3\text{P}_0$ lifetime listed in Table 6 is 377 s, but the result obtained from the formula in the inset to Fig. 3 is 19.5 s, which is close to the observed value.
- [26] E. Peik, G. Hollemann, and H. Walther, Phys. Rev. A **49**, 402 (1994).